Topological Characterization of Three-Electron-Bonded Radical Anions

Isabelle Fourré,*,† Bernard Silvi, Alain Sevin, and Hilaire Chevreau

Laboratoire de Chimie Théorique, Université Pierre et Marie Curie, UMR-CNRS 7616, 4 place Jussieu, 75252 Paris Cedex 05, France

Received: August 7, 2001; In Final Form: November 6, 2001

The three-electron bond in radical anions of the $H_nXYH_m^-$ type, with X, Y = Cl, S, P, Si, F, O, N, C and *n*, *m* = 0−2, has been investigated from the topological analysis of the electron localization function (ELF) at the BH&HLYP level. It is shown that the topological modifications arising within the bonding region upon vertical electron attachment are of three different types, according to the vertical electron affinity (vEA) of the neutral compound: for vEA smaller than −16 kcal mol^{-1} the bonding population remains unchanged, as in H_4P_2, for negative vEA greater than −16 kcal mol^{-1} the bonding population decreases, as in H_2S_2, and for positive vEA the bonding population disappears, as in Cl_2. However, after relaxation of the geometry, the formation of the three-electron bond is accompanied in all cases by the disappearance of the X−Y bonding basin (which is the signature of the covalent bond in the neutral parent molecule). From a quantitative point of view, the topological approach also allows us to characterize the transfer of charge and spin densities that arises upon these processes toward the lone pairs basins of the X and Y atoms. Finally, to quantify the electron fluctuation between the two moieties, an index of delocalization has been defined from the analysis of the variance of the lone pairs population. This index increases approximately linearly with the dissociation energy D_e of the radical anions, provided that they are separated into a group of weakly bonded ones (D_e < 18 kcal mol^{-1}) and a group of strongly 3e-bonded ones (D_e > 18 kcal mol^{-1}).

I. Introduction

Since the past fifteen years, a growing interest has been noted in the nature and stability of two-center−three-electron (2c−3e or 3e) bonds that play an important role in radical and electron-transfer chemistry. Some typical 3e-bonded radical anions are found in the series of dihalogen anions such as F_2^- and Cl_2^-,[1] which are known to exhibit significant bonding energies relative to the separate products (around 30 kcal mol^{-1}). First described by Pauling[2] in 1931 in the context of the valence bond model of the chemical bond, the 3e bond has been further studied both in valence bond (VB) and molecular orbital (MO) theories. In VB theory,[2−11] the 3e bond between two fragments A and B is viewed as arising from a stabilizing resonance between two limiting Lewis structures, as $\ddot{A}\dot{B} \leftrightarrow \dot{A}\ddot{B}$ (in which atomic formal charges have been omitted). The closer are the energies of the two resonating structures, the greater is the resonance energy.[10] In MO theory[4−6,8−10,12−17] two electrons occupy a bonding MO, Ψ_{ab}, whereas a third one occupies the antibonding counterpart, Ψ^*_{ab}, thus leading to a formal bond order of a maximum of $^1/_2$ (when A = B), similar to the one-electron bond. The equivalence between MO and VB descriptions of the 3e bond has recently been revisited by Harcourt[6] and can be illustrated by the orbital diagrams displayed in Figure 1.[18] The Linnett $(a)^1(\Psi_{ab})^1(b)^1$ configuration, where a and b are the atomic orbitals centered on A and B, respectively (see diagram (2) of Figure 1), involves parallel spin for the nonbonding a and b electrons, thus resulting in a net destabilizing interaction. The bonding results solely from the (shared) Ψ_{ab} electron, whose spin is opposed to the spin of each of the a and b electrons. According to Harcourt,[18,19] this justifies the choice of the Linnett VB structure[20] $\dot{A}\cdot\dot{B}$ (with spin $\dot{A} \times \dot{B}$, × for $m_s = {}^1/_2$, ○ for $m_s = -{}^1/_2$) to represent the 3e bond, instead of A···B (Pauling), A−$\dot{B}$ or A∴B, the latter continuing to be used very widely.

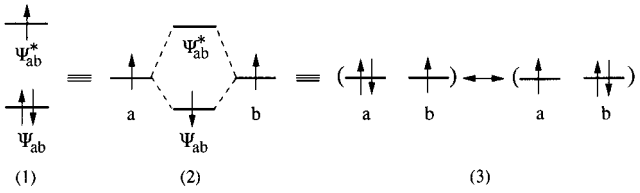

Figure 1. Orbital diagrams (for A = B) associated with (1) the MO configuration $(\Psi_{ab})^2(\Psi^*_{ab})^1$, (2) the Linnett configuration $(a)^1(\Psi_{ab})$-$1(b)^1$, and (3) the VB type wave function $(a)^1(b)^2 + (a)^2(b)^1$, which are equivalent when two atomic orbitals are used to accommodate the three electrons (the identity between configurations (1) and (2) was deduced by Linnett[62]).

Among the numerous theoretical studies that have dealt with the 3e bond, several are focused on its nature on a rather fundamental point of view. Their common objective has been to extract some chemical information from the output of traditional ab initio or DFT calculations. Gill and Radom have shown that electron correlation is essential in the calculations of (2c−3e) dissociation energies within MO theory.[9] However, they also use the simple Hückel approximation with overlap to find the optimal value of the overlap between the atomic orbitals involved in the 3e bond. In the same spirit, the VB theory aims to provide wave functions that possess more chemical meaning than those calculated in the MO theory framework, owing to their compactness. The breathing orbital valence bond (BOVB) method of Hiberty et al.,[21] in which the orbitals are allowed to follow the instantaneous charge fluctuation by rearranging in size and shape, enables us to describe the 3e bond in terms of only two configurations (corresponding to the resonant orbital

† E-mail: fourre@lct.jussieu.fr.

10.1021/jp013054j CCC: $22.00
Published on Web 02/13/2002

diagrams (3) of Figure 1).[7] However, the BOVB method being CPU time-consuming, Hiberty et al. proposed the so-called "uniform mean-field HF procedure", in which the BOVB method is used a posteriori to correct the dissociation energy that was found to be too small.[8] Other theoretical studies carried out in the framework of MO theory have been using simple VB or Hückel models to interpret the results of their calculations.[4,5,12,17] Alternatively, Bieckelhaupt et al. analyzed the nature of the 3e bond in $H_2S_2^+$ within DFT using a quantitative energy decomposition scheme.[14]

Except for the latter one, the aforementioned studies illustrate, through the resort of qualitative VB analysis, the need for a local representation of the 3e bond (and generally of the chemical bonding). Actually, this analysis leads to a compact representation *of the wave function* associated to the bond, but not *of the bond*, since the latter is not an observable in the sense of quantum mechanics. To deal with the concepts of bond and of the electron pair that are so useful in chemistry, one has to start from the valence theory of Lewis,[22] and also from the VSEPR model of Gillespie, which is the natural development of the Lewis theory toward the prediction of molecular geometry.[23,24] The topological theories of the chemical bonding aim to provide a mathematical model of the Lewis theory. In these theories, one extracts the chemical concepts from the mathematical properties of the gradient vector field of a local function $f(\mathbf{r})$, called the potential function. In the theory of atoms in molecules (AIM) of Bader[25] the electron density function $\rho(\mathbf{r})$ is used as a potential function that enables us to partition the molecular space into atomic basins and to rigorously define concepts such as *atom in a molecule*, *bond path*, and *molecular structure*. Bader et al.[26−28] and MacDougall[29] have also examined the Laplacian of the electron density in order to evidence the electron pairing that does not emerge from the gradient field of $\rho(\mathbf{r})$, although it is a central idea in the valence theory of Lewis.[22] However, they did not fully extend the topological approach to this quantity.[30]

An alternative choice of potential function, made by Silvi and Savin,[31] uses the Electron localization function (ELF) introduced by Becke and Edgecombe.[32] As shown in a review of Savin and co-workers,[33] ELF provides a qualitative description of the electron localization that is almost independent of the theoretical method used to calculate it. The topological analysis of the gradient field of ELF enables a partition of molecular space that is consistent with the chemical sense, namely into cores, bonds, and lone pairs *basins*. Quantities associated with these regions, such as integrated charge or spin density can be calculated and interpreted. A powerful tool for the description of chemical bonding is thus obtained, as shown in many systems.[34−46] A theory of chemical reactions has also been developed, based on catastrophe theory,[47] in which the evolution of the gradient field of ELF is studied as a function of a set of control parameters. At the present state of the art the theory only deals with bond breaking and bond formation, for which the control space parameters (the nuclear coordinates) undergo continuous variations. However, there exist phenomena for which the control space parameters undergo discrete variations, i.e., electronic excitation, ionization, and electron attachment. We have recently proposed a preliminary analysis of the bonding evolution occurring during these processes, in which we analyzed the topological changes undergone first upon each vertical process and second upon relaxation of the geometry.[35] In the present work, we follow a similar approach for the electron attachment on a molecule, giving rise to a 3e-bonded radical anion. This process induces a strong perturbation to the electron localization function because it corresponds to a local change of the electron pairing. One thus expects a catastrophe to occur, i.e., a change in the number and nature of the basins of the ELF gradient field. Actually, this prediction has already been confirmed and specified by two recent studies: in the former, Krokidis et al. investigated the charge-transfer reaction $Li + Cl_2 \rightarrow Li^+ + Cl_2^-$,[48] in the latter, dealing with the stability of disulfide radicals, Bergès et al. examined the effect of an electron attachment on H_2S_2.[49] In both cases, the topology of the radical anions does not present any bonding basin, which is the signature of the covalent bond in the neutral molecule. The aim of the present work is to investigate the nature of the 3e bond by means of topological tools, to determine the qualitative characteristics of this type of bonding. Very accurate wave functions are generally useless to extract reliable topological pieces of information; nevertheless, the calculations should give rise to (i) the correct electronic state, (ii) a geometry in agreement with the available experimental results or those of the best calculations (a few percent of ångstroms on the distances and a few degrees on the angles are enough), and (iii) the order of magnitude of the dissociation energy. For this purpose we have studied the electron attachment on three series of molecules of the H_nXYH_m type: the isoelectronic to Cl_2 ones (i.e., with X, Y = Cl, S, P, Si and n, m taking the proper values between 0 and 2), the isoelectronic to F_2 one (i.e., X, Y = F, O, N, C), and the isoelectronic to ClF one. On a more quantitative point of view, we expect to better understand the transfer of charge and spin densities resulting from the reorganization of the basins, as well as to characterize the electron fluctuation, which is a central phenomenon in this hemibonded compounds. The results obtained within the topological approach have been compared to the descriptions provided by the MO and VB theories.

II. Topological Analysis of the ELF Gradient Field

The topology of the gradient vector field of a local function $f(\mathbf{r})$ is fully defined by its critical points, i.e., the points at which $\nabla f(\mathbf{r}) = 0$, whereas the noncritical points define the equivalent of trajectories. The critical points are of three types, namely the local maxima, also called attractors, the local minima, and the saddle points. The set of points corresponding to trajectories ending at a given attractor is named the basin of this attractor and the separatrices are the bounded surfaces between the basins (for a comprehensive introduction to the theory of the gradient dynamical systems, see the textbook of Abraham and Shaw[50]). This treatment is applied to the electron localization function, originally derived by Becke and Edgecombe to provide an orbital independent description of the electron localization. The original derivation considers the Laplacian of the conditional probability of finding an electron at the position r_1 when a first electron of same spin is already in r_2, $\nabla^2 P(r_1,r_2)_{r_1=r_2}$. Savin et al.[33] have highlighted its physical meaning by expressing it in terms of the increase of the local kinetic energy density due to the Pauli repulsion $T_s(\mathbf{r}) - T_{vW}(\mathbf{r})$:

$$\eta(\boldsymbol{r}) = \left[1 + \left(\frac{T_s(\mathbf{r}) - T_{vW}(\mathbf{r})}{T_{TF}(\mathbf{r})}\right)^2\right]^{-1} \qquad (1)$$

where $T_s(\mathbf{r})$ is the positive definite kinetic energy density and $T_{vW}(\mathbf{r})$ and $T_{TF}(\mathbf{r})$ are respectively the von Weiszäcker and the Thomas−Fermi kinetic energy functionals of the actual system. ELF is close to 1.0 in the regions where the Pauli repulsion is weak, thus dominated by an electron pair (or a lone electron) behavior, and the value 0.5 corresponds to that of a homoge-

neous electron gas. Alternatively, to explore the orbital underpinnings of ELF, Burdett and McCormick[51] have proposed an interpretation of the function based upon the nodal properties of the occupied orbitals in a system.

The organization of the basins in the molecular space provides a representation of the bonding that is consistent with the familiar Lewis theory. There are two kinds of basins, on one hand the core basins noted C(X) that encompass the nuclei X with $Z > 2$, on the other hand the valence basins V(X,Y,...) that fulfill the remaining space. The valence basins are characterized by their synaptic order, i.e., the number of core basins with which they share a common separatrice. Monosynaptic basins thus correspond to conventional lone pairs, disynaptic ones to two-center bonds, polysynaptic ones to multicenter bonds. Asynaptic basins, i.e., sharing no separatrices without any core basins, may eventually exist in transient states (such as those occurring upon vertical electron attachment).

Of course, quantitative properties can also be obtained with ELF, by integrating the related property densities over the basins. For example, the average population of a given basin Ω_a is defined by

$$\bar{N}(\Omega_a) = \int_{\Omega_a} \rho(\mathbf{r})\, d\mathbf{r} \tag{2}$$

where $\rho(\mathbf{r})$ denotes the one electron density at $\mathbf{r}$ and Ω_a is the volume of the basin. When dealing with open-shell systems of particular importance are the integrated basin spin densities:

$$\langle S_z \rangle_{\Omega_a} = \frac{1}{2} \int_{\Omega_a} (\rho^{\alpha}(\mathbf{r}) - \rho^{\beta}(\mathbf{r}))\, d\mathbf{r} \tag{3}$$

In this study, it is also worthwhile to calculate the variance of the basin population:

$$\sigma^2(\bar{N},\Omega_a) = \int_{\Omega_a} d\mathbf{r}_1 \int_{\Omega_a} \pi(\mathbf{r}_1,\mathbf{r}_2)\, d\mathbf{r}_2 + \bar{N}(\Omega_a) - [\bar{N}(\Omega_a)]^2 \tag{4}$$

where $\pi(\mathbf{r}_1,\mathbf{r}_2)$ is the spinless pair function. In contrast to $\bar{N}(\Omega_a)$ and $\sigma^2(\bar{N},\Omega_a)$, the square root of the variance, $\sigma(\bar{N},\Omega_a)$, cannot be defined by an operator and therefore its interpretation in terms of quantum-mechanical standard deviation is not fully consistent (in particular, the absolute value of $\sigma(\bar{N},\Omega_a)$ can be larger than $\bar{N}(\Omega_a)$). The relative fluctuation of the basin population has been introduced by Bader,[52] and its generalization to localization basins,

$$\lambda(\bar{N};\Omega_a) = \frac{\sigma^2(\bar{N},\Omega_a)}{\bar{N}(\Omega_a)} \tag{5}$$

provides an indication of the delocalization within the Ω_a basin. It has been shown that the variance of the population of a given basin can be readily written as a sum of contributions arising from the others basins:[34]

$$\sigma^2(\bar{N},\Omega_a) = \sum_{b \neq a} \bar{N}(\Omega_a)\, \bar{N}(\Omega_b) - \bar{N}(\Omega_a,\Omega_b) \tag{6}$$

$$= \sum_{b \neq a} B_{\Omega_a,\Omega_b} \tag{7}$$

In this expression $\bar{N}(\Omega_a)\, \bar{N}(\Omega_b)$ is the number of electron pairs classically expected from the basin population, i.e., assuming that there is no interaction between the basins Ω_a and Ω_b, whereas $\bar{N}(\Omega_a,\Omega_b)$ is the actual number of pairs obtained by integration of the quantum mechanical pair density over the basins Ω_a and Ω_b, thus taking into account their interaction. Therefore this alternative expression of the variance gives a natural picture of the electron delocalization. The larger is the B_{Ω_a,Ω_b} term, the larger is the delocalization of the electrons referenced to basin Ω_a into basin Ω_b. When divided by $\sigma^2(\bar{N},\Omega_a)$, this contribution is obtained in percentage (we shall refer it as "relative B_{Ω_a,Ω_b}"). A similar covariance analysis is now currently carried out in the AIM approach[53] and, as pointed out by Chesnut and Bartolotti,[54] our B_{Ω_a,Ω_b} corresponds to the negative of the F(B,A) term of Fradera et al.[53] These latter authors define a delocalization index $\delta_{A,B}$ as the sum of the magnitudes of F(B,A) and F(B,A). It provides a quantitative indication of the importance of the electron delocalization between the atomic basins A and B. A few years before the publication of Fradera's paper, Ángyán et al.[55] revisited the topological bond orders of Cisolowski and Mixon[56] and proposed an expression of the bond order that is formally identical to $\delta_{A,B}$. The bond order interpretation, which relies on the projection of the wave function onto a limited (incomplete) set of atomic orbitals, has a much weaker epistemological status than the statistical one in terms of covariance. Nevertheless, a fair correlation is often observed[54] between $\delta_{A,B}$ and the disynaptic basin population N(V(A,B)) (roughly N(V(A,B)) = $2\delta_{A,B}$) involving the same atomic centers. In this paper, we introduce an interbasin delocalization index $\delta_{\Omega_a,\Omega_b}$ that is consistent with the definition of Fradera et al.

$$\delta_{\Omega_a,\Omega_b} = B_{\Omega_a,\Omega_b} + B_{\Omega_b,\Omega_a} \tag{8}$$

III. Computational Method

At the present state of the art, the topological analysis of the ELF gradient field requires a wave function written with a single determinant (HF or DFT). Unfortunately, the most commonly used density functionals (including B3LYP) systematically fail to describe quantitatively the two-center three-electron systems, by overestimating the binding energies and the equilibrium distances, as shown recently by Braïda et al.[15] The inadequacy of the current DFT methods is attributed to an overestimation of the self-interaction part of the exchange energy of the hemibonded ions due to their delocalized electron hole. Nevertheless, the BH&HLYP hybrid functional, which includes 50% (exact) Hartree−Fock exchange (thus correcting for self-interaction) provides rather good agreement with the MP4 or CCSD(T) calculations of the dissociation energy. The optimizations of the geometries, as well as the calculations of the wave functions of the systems under scrutiny, have thus been done at the hybrid density functional BH&HLYP[32] level, within the spin-unrestricted formalism, in the standard 6-311++G(3df,2p) basis set, and by using the Gaussian94 software.[57]

The Gaussian wfn output was then used as an input of the TopMod package of programs developed in our laboratory,[58] which performs the calculation of the ELF function on a grid as well as the various steps of the topological analysis described above.

IV. Results and Discussion

IV.A. Structural Properties. The geometry of the H_nXYH_m systems and of their associated radical anions has been fully optimized. The structures of the compounds with X, Y = Cl, S, P, Si are shown in Figure 2, together with pertinent geometrical data. First of all, limiting oneself to the neutral systems, the (nearly systematic) lengthening of the X−Y bond distance when X goes from the right to the left of the periodic table is consistent with the decrease of the electronegativity of

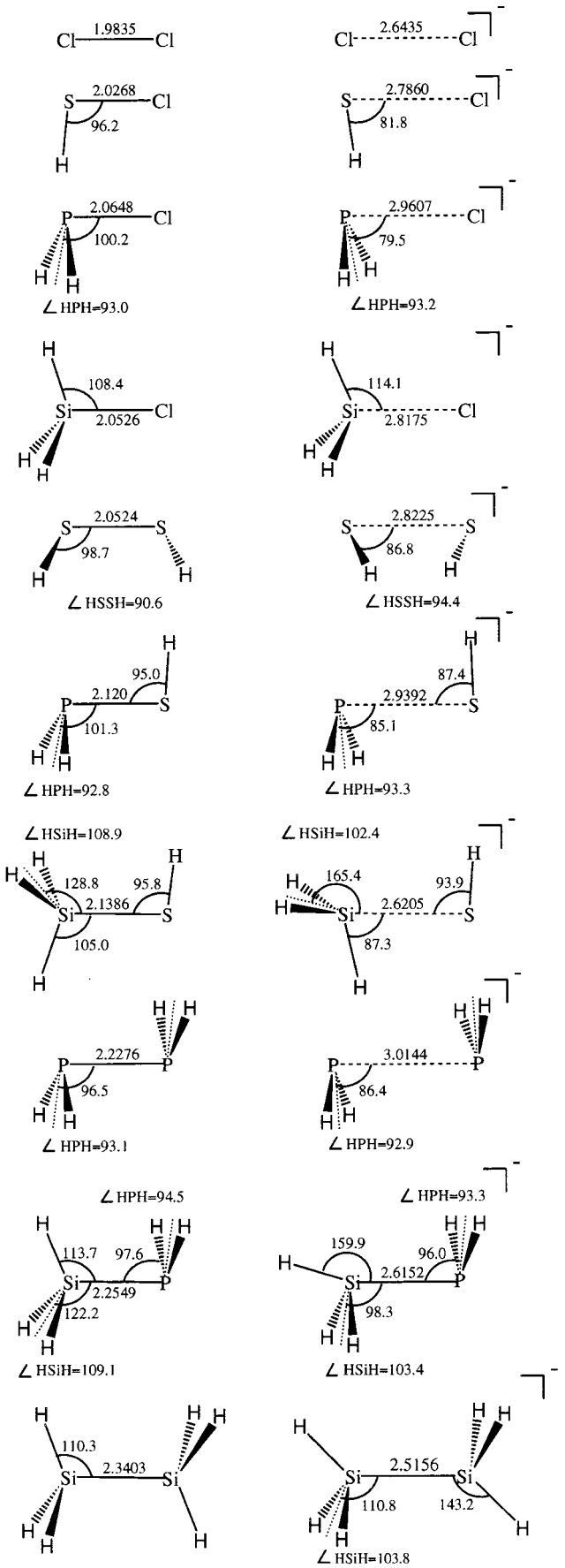

Figure 2. BH&HLYP-optimized structures for H_nXYH_m systems (left-hand side) and their associated radical anions (right-hand side), with X, Y = Cl, S, P, Si and n, m = 0−2. The 6-311++G(3df, 2p) basis set was used for all the systems. Distances are in angstroms and angles are in degrees.

TABLE 1: Dissociation Energy (kcal mol^{-1}) for the H_nXYH_m Molecules Isoelectronic to Cl_2 and for the Associated Radical Anions, Labeled by "a(3e)" When the X and Y Atoms Are Held Together by a Three-Electron Bond and by "a" If Not (See Text)

species	symm[a]	B3LYP	BH&HLYP
Cl_2	$D_{\infty h}$	57.6	49.8
a(3e)		37.1	30.7
HSCl	C_s	64.8	58.9
a(3e)		20.1	15.3
H_2PCl	C_s	79.6	76.0
a(3e)		11.1	8.5
H_3SiCl	C_{3v}	110.7	104.8
a(3e)		13.3	10.3
H_2S_2	C_2	64.4	59.8
a(3e)		30.7	26.0
H_2PSH	C_s	67.4	64.5
a(3e)		16.8	13.5
H_3SiSH	C_s	88.3	87.7
a(3e)		20.6	18.0
H_4P_2	C_{2h}	57.9	55.8
a(3e)		24.4	21.0
H_3SiPH_2	C_s	72.6	71.2
a		29.2	27.2
H_6Si_2	D_{3d}	72.6	74.1
a	C_{2h}	29.6	28.7

[a] Unless otherwise specified, the neutral compound and its anion have the same symmetry.

X (this is particularly accentuated for the series of symmetrical homonuclear compounds $Cl_2 \rightarrow H_2S_2 \rightarrow H_4P_2$). Note, however, that the Si−S and Si−P bond distances increase less than expected with respect to the P−S and P−P distances, respectively, and that the Si−Cl distance is even slightly smaller than the P−Cl one. The evolution of the ∠HXY angle when X varies can be understood using the VSEPR model (for example, it decreases from ∼109° in H_3SiCl to ∼96° in HSCl, in agreement with the increase of the X lone pairs, which stands in a tetrahedral environment). When an electron is attached to the system, the most dramatic effect on the geometry is the lengthening of the bond distance (which is the geometrical parameter of interest to characterize the 3e bond), from about 0.6 Å for Cl_2^- (i.e., a lengthening of about 30%) to 0.9 Å for H_2PCl^- (i.e., a lengthening of about 43%). This is consistent with the decrease of the formal bond order from 1 to $^1/_2$, arising from the description of the process in terms of the MO theory. It is worthy to note that, for a series of radical anions with a given Y atom (for example, H_nXCl^-), the bond distance increases when X goes from Cl to P, but then systematically decreases from P to Si. Finally, in most cases, the ∠HXY (and ∠HYX) angles are smaller than in the neutral system, due to the increase of the electronic density in the X (and Y) lone pairs. Nevertheless, in H_3SiSH^-, two of the ∠HSiS angles increase (those which are "cis" with respect to the SH group) and the third one ("trans") decreases, in agreement with the "cis" localization of the "lone pair" of Si (actually containing only one electron). A similar evolution is observed for the ∠HSiP angles of $H_2PSiH_3^-$.

Another spectroscopic parameter of interest is the dissociation energy D_e of the X−Y bond, which has been calculated, for the neutral molecules isoelectronic to Cl_2 and their radical anions, at the B3LYP and BH&HLYP levels and is reported in Table 1. Except for Cl_2, and in a lesser extent, for HSCl and H_2S_2, the two DFT methods give rise to similar results for the neutral, but, as mentioned previously, the half and half method is to be preferred for the 3e-bonded anions. Indeed, the experimental dissociation energy of Cl_2^- is 31.8 kcal mol^{-1}, which compares better with the BH&HLYP value (30.7) than

TABLE 2: BH&HLYP/6-311++G(3df,2p) Calculations for the H_nXYH_m Molecules Isoelectronic to ClF and for the Associated Radical Anions

species	symm[a]	D_e[b]	R_e[c]
FCl	$C_{\infty v}$	49.5	1.609
a(3e)[a]		26.5	2.212
H_3CCl	C_{3v}	83.1	1.777
a[a]		0.7	3.456
HSF	C_s	75.3	1.608
a(3e)		26.1	2.223
HOSH	C_1	76.6	1.646
a(3e)		15.1	2.459
H_2NSH	C_s	64.7	1.681
a		9.8	3.538
H_3CSH	C_s	74.1	1.807
a(3e)		1.0	3.496
H_2PF	C_s	108.3	1.598
a(3e)		22.9	1.990
H_3CPH_2	C_s	72.6	1.846
a		2.5	3.406

[a] See Table 1. [b] Dissociation energy, in kcal mol^{-1}. [c] X−Y bond equilibrium distance, in Å.

TABLE 3: BH&HLYP/6-311++G(3df,2p) Calculations for the H_nXYH_m Molecules Isoelectronic to F_2 and for the Associated Radical Anions

species	symm[a]	D_e[b]	R_e[c]
F_2	$D_{\infty h}$	16.0[d]	1.357
a(3e)		30.0[d]	1.940
H_3CF	C_{3v}	109.8	1.369
a		3.3	2.640
H_2O_2	C_2	39.9	1.409
a(3e)		25.3	2.305
H_4N_2	C_{2h}	62.0	1.453
a(3e)		18.5	2.588

[a] See Table 1. [b] Dissociation energy, in kcal mol^{-1}. [c] X−Y bond equilibrium distance, in Å. [d] Experimental values: 36.9 kcal mol^{-1} for the neutral molecule, 30.2 kcal $mol^{-1}$for the radical anion.[1]

with the B3LYP one (37.1), whereas for the neutral compound the B3LYP value is actually closer to the experimental one (58.1 kcal mol^{-1})[1]. Consistent with the lengthening of the X−Y bond, one observes a decrease of D_e upon electron attachment, which ranges from a factor of 1.7 for Cl_2 up to a factor of 10 for H_3SiCl. For a series of anions such as H_nXCl^-, a remark similar to the one concerning the bond distance can be made for the variation of the dissociation energy.

Among the compounds isoelectronic to ClF (respectively to F_2), only seven (respectively four) give rise to stable anions involving a direct interaction between the heavy atoms, and are thus possible candidates for the formation of a 3e bond. For the sake of compactness, the dissociation energy and the X−Y bond distance of the neutral molecules and of the associated radical anions are reported in Tables 2 and 3, respectively. The inability of the BH&HLYP method to reproduce the experimental D_e of F_2 should be noted, even though, as will be seen in the following section, the resultant topological description is the same as the one obtained by Llusar et al. from a B3LYP calculation.[37] In contrast with the isoelectronic to Cl_2 systems, it is worthy to note the very large increase of the X−Y bond distance upon electron attachment for all systems containing CH_3 groups (∼+1.3 Å for H_3CF^- and ∼+1.7 Å for H_3CCl^-, $HSCH_3^-$, and $H_2PCH_3^-$) and also for $HSNH_2^-$ (+1.8 Å), compared to those of the isoelectronic to Cl_2^- compounds (never greater than 0.9 Å). Except for $HSNH_2^-$, the associated dissociation energies are very below the commonly accepted lower limit for the existence of a 3e bond (∼15 kcal mol^{-1}). We will see in the following section how the ELF topology of these very weakly bonded anions differs from the ELF topology of the other ones. Finally, among the stable anions that are not 3e-bonded, we found hydrogen-bonded ones, as HOF^- and H_2NF^-, whereas in $H_2NCH_3^-$ the electron is simply trapped into a Rydberg orbital (indeed, the N−C bond distance is identical to the neutral one).

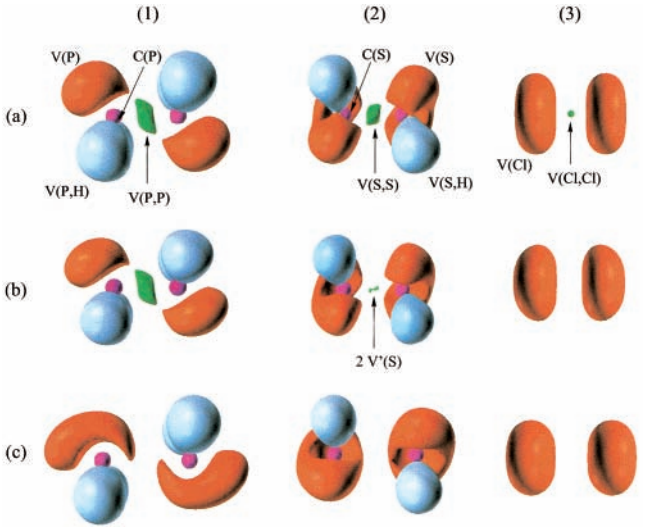

Figure 3. ELF=0.8 isosurfaces for the H_nX_{2n} compounds (a) and their associated vertical (b) and relaxed (c) radical anions: (1) H_2S_2; (2) H_4P_2; (3) Cl_2. Color code: magenta = core, red = valence monosynaptic, blue = valence protonated, green = valence disynaptic.

IV.B. Topological Description of the Three-Electron Bond. As mentioned previously, this analysis involves first the partition of the molecular space into basins, which provides a qualitative description of the chemical bonding, second the calculation of quantitative properties, such as the basin population and its variance, as well as the basin-integrated spin density. From this procedure, our aim is to obtain information about the topological features of the 3e bond and electron delocalization, which plays a central role in this type of bonding. Section IV.B.1 is devoted to the analysis of the topological modifications undergone by the systems under scrutiny, upon vertical attachment and upon geometry relaxation of the vertical anion (i.e., variation of the number of basins and of the basin-integrated properties). Section IV.B.2 is more specifically devoted to the topological characterization of the delocalization in 3e bonds.

IV.B.1. Analysis of the Electron Attachment Process. Following the same procedure as in the discussion of the structural properties, we will analyze in detail the results concerning the systems isoelectronic to Cl_2, and more briefly those concerning the systems isoelectronic to F_2 or to ClF. Figure 3 shows the ELF = 0.8 localization domains of the symmetrical $H_{2n}X_2$ species (with (X, *n*) = (Cl, 0), (S, 1), (P, 2)), of their associated vertical radical anions and of the 3e-bonded radical anions. We will see below that they correspond, from a topological point of view, to three different mechanisms of 3e bond formation.

Neutral Molecules. The topology of the $H_{2n}X_2$ neutral molecules (see panels a of Figure 3) are composed of the following: (i) two core basins C(X) and C(X′); (ii) 2*n* protonated disynaptic basins V(X,H), each associated with the electronic pair of a X−H bond; (iii) as expected from the Lewis representation of these molecules, 6 − 2*n* monosynaptic basins V(X), each related to a lone electron pair (this rule is valid for H_4P_2 and H_2S_2, but in Cl_2 the lone pairs of each atom are gathered in a single basin V(Cl) by the cylindrical symmetry); (iv) one disynaptic V(X,X′) basin, which demonstrates the

TABLE 4: Basins Population, $\bar{N}$, Standard Deviation, $\sigma(\bar{N})$, Relative Fluctuation, $\lambda(\bar{N})$, and Contribution of Other Basins (%) to $\sigma^2(\bar{N})$ for $H_{2n}X_2$ Molecules

basin	$\bar{N}$	$\sigma(\bar{N})$	$\lambda(\bar{N})$	contribution analysis
				H_4P_2
$C(P_1)$	10.1	0.21	0.05	$V(P_1)$ 38%, $V(P_1,P_2)$ 21%, $V(H_1,P_1)$ 16%
$V(H_1,P_1)$	2.0	0.78	0.31	$V(H_2,P_1)$ 23%, $V(P_1,P_2)$ 20%, $C(P_1)$ 16%
$V(P_1,P_2)$	1.8	0.99	0.55	$V(P_1)$ 18%, $V(H_1,P_1)$ 12%
$V(P_1)$	2.1	0.93	0.41	$V(H_1,P_1)$ 24%, $V(P_1,P_2)$ 21%, $C(P_1)$ 20%
				H_2S_2
$C(S_1)$	10.1	0.71	0.05	$V(S_1)$ 65%, $V(H_1,S_1)$ 18%, $V(S_1,S_2)$ 12%
$V(H_1,S_1)$	1.9	0.84	0.37	$V(S_1)$ 66%, $C(S_1)$ 13%, $V(S_1,S_2)$ 11%
$V(S_1,S_2)$	1.5	0.96	0.63	$V(S_1)$ 35%
$V(S_1)$	4.3	1.2	0.32	$V(H_1,S_1)$ 34%, $C(S_1)$ 25%, $V(S_1,S_2)$ 24%, $V(S_2)$ 12%
				Cl_2
$C(Cl_1)$	10.1	0.75	0.06	$V((Cl_1)$ 88%
$V(Cl_1,Cl_2)$	1.0	0.86	0.73	$V((Cl_1)$ 44%
$V(Cl_1)$	6.4	1.1	0.19	$C(Cl_1)$ 42%, $V(Cl_2)$ 29%, $V(Cl_1,Cl_2)$ 27%

TABLE 5: BH&HLYP/6-311++G(3df,2p) Calculations (kcal mol^{-1}) for the H_nXYH_m Molecules

species	vEA[a]	aEA[b]	species	vEA[a]	aEA[b]	species	vEA[a]	aEA[b]
Cl_2	16.8	61.1	FCl	6.8	57.4	F_2	−7.1	79.6
HSCl	−2.1	37.8	HSF	−12.8	19.3			
H_2PCl	−14.5	14.8	H_2PF	−20.5	−15.2			
H_3SiCl	−24.1	−15.6	H_3CCl	−18.5	0.7	H_3CF	−20.2	−35.4
H_2S_2	−15.7	15.4	HOSH	−16.1	2.2	H_2O_2	−29.3	14.7
H_2PSH	−18.7	−0.9	H_2NSH	−16.5	−4.6			
H_3SiSH	−19.5	−18.7	H_3CSH	−20.7	−22.0			
H_4P_2	−17.6	−10.3				H_4N_2	−30.0	−35.7
H_3SiPH_2	−19.1	−19.1	H_3CPH_2	−18.3	−44.1			
H_6Si_2	−22.1	−19.4						

[a] Vertical electron affinity (i.e., using the energy of the vertical anion). [b] Adiabatic electron affinity (conventional electron affinity).

covalent character of the X−X′ bond. The basin populations, as well as the analysis of the variance are presented in Table 4. For H_2S_2, the two monosynaptic basins of each S atom have been merged for simplicity. The decrease of the V(X,X′) population (1.8 in H_4P_2, 1.5 in H_2S_2, and 1.0 in Cl_2), and the concomitant increase of the V(X) population (2.1 in H_4P_2, 4.3 in H_2S_2, and 6.4 in Cl_2) illustrates the increasing ionic character of the bond. An additional information is provided by the analysis of the variance of the V(X,X′) population: it is rather large in H_4P_2 (0.55 vs 0.40 for a conventional covalent bond), the most important contributions arising from the lone pairs (18%). As the covalent character of the bond weakens, the relative fluctuation increases (0.63 for H_2S_2 and 0.71 for Cl_2) as well as the lone pair contributions (35% for H_2S_2 and 44% for Cl_2). Among the other systems considered in this work, the particularity of F_2 is noteworthy (see Table 8). It presents two monosynaptic V′(F) and V′(F′) basins (in place of the expected V(F,F′) one) centered on the axis linking the two fluorine cores, each containing 0.18 *e*. This is the signature of a "protocovalent" bond, as first described by LLusar et al. in their study of homopolar depleted bond.[37]

Vertical Anions. Upon vertical electron attachment, three different topological behaviors are observed in the valence region:

- no evolution, as in H_4P_2;
- a decrease of the V(X,Y) population, which may be associated, as in H_2S_2, with a splitting of the disynaptic V(X,Y) basin into two monosynaptic basins V′(X) and V′(Y);
- a disappearance of the disynaptic V(X,Y) basin, as in Cl_2;

Panels b of Figure 3 illustrate these topological modifications from a qualitative point of view, whereas quantitative properties such as valence basin populations ($\bar{N}$), integrated spin densities ($\langle S_z \rangle$), and variation of the number of basins with respect to the neutral molecule ($\Delta\mu$), can be found in Table 6. At first glance, it seems that the lower the population of the V(X,Y) basin in the neutral molecule, the more accentuated is its lowering upon vertical attachment, with eventually the disappearance of the basin. However, as shown by Table 7 (respectively, by Table 8), the population of the V(X,Y) basins in compounds isoelectronic to ClF (respectively, isoelectronic to F_2) does not range between the same values as in compounds isoelectronic to Cl_2, so that the type of topological change arising upon vertical attachment cannot be correlated to this population, at least in an absolute way. Alternatively, the value of the vertical electron affinity (vEA) seems to govern the topological changes undergone in the course of this transient process.

1. Compounds for which vEA is smaller than roughly −16.0 kcal mol^{-1} retain their V(X,Y) basin under vertical attachment, without modification of their population, as H_4P_2, or with a very small lowering. Other molecules isoelectronic to Cl_2 belonging to this set are H_3SiCl, H_2PSH, H_3SiSH, H_2PSiH_3, and H_6Si_2, as shown by the data reported in Tables 5 and 6. It is noteworthy that the adiabatic electron affinity (aEA) of these species has also a negative value (i.e., the relaxation does not successfully stabilize the anions with respect to their parent neutral molecule). The only observation of the ELF = 0.8 isosurface of vertical $H_4P_2^-$ makes us think there is no variation of the number of basins under vertical attachment (i.e., no catastrophe) but, actually, only half of the extra electron density locates itself in the existing valence basins: the monosynaptic ones absorb only 2×0.1 *e* and the disynaptic protonated ones around 4×0.07 *e* each (it has been observed that the maximum population of a V(X,H) basin is around 2.1 *e*). The remaining 0.5 *e* is distributed among four newly created asynaptic basins. In the framework of catastrophe theory such a process in which $\Delta\mu$ is positive is called a *plyomorphic* process. However, the attractors of these basins are located far from the bonding region, beyond the V(P,H) basins.[59] The associated electron density is thus described to a great extent by Rydberg orbitals and is therefore not really captured by the molecule. The basin-integrated spin densities, also reported in Table 6, confirm the nearly equal sharing of the extra electron density between the valence (monosynaptic plus protonated) and asynaptic basins (note that the sum of the spin density is not exactly equal to 0.5, because the small contributions of the core are not indicated). The contribution of the asynaptic basins increases more or less as the vEA decreases (except for the vertical anion H_3SiCl^-), up to a population of 0.7 *e* and an integrated spin density of 0.31 in the vertical anion $H_6Si_2^-$. As for the compounds isoelectronic to ClF (respectively to F_2), all but ClF and HSF (respectively, all but F_2) behave as H_4P_2 upon electron attachment, as shown by the data reported in Tables 5 and 7 (respectively, in Tables 5 and 8). The increasing contribution of the asynaptic basins to the population and to the integrated spin density in vertical anions, as the total number of electrons decreases, is noteworthy, as illustrated by the series H_3SiCl^- ($\bar{N} = 0.5$; $\langle S_z \rangle = 0.22$) → H_3CCl^- ($\bar{N} = 0.7$; $\langle S_z \rangle = 0.32$) → H_3CF^- ($\bar{N} = 0.8$; $\langle S_z \rangle = 0.35$).

2. For compounds whose vEA verifies −16.0 < vEA (kcal mol)$^{-1}$ < 0, the vertical attachment gives rise to a decrease of the V(X,Y) population. This set includes the H_2S_2 molecule but also the isoelectronic systems HSCl and H_2PCl. Note that their aEA is positive; i.e., they are stable with respect to the neutral state. In H_2S_2, one actually observes the splitting of the V(S,S′) basin into two monosynaptic V′(S) and V′(S′) basins. These

TABLE 6: Valence Basin Populations, $\bar{N}$, for the Neutral Ground State, the Vertical Anion (va), and the Relaxed Anion (a), Where (3e) Means "Three-Electron-Bonded", for H_nXYH_m Molecules (X, Y = Cl, S, P, Si; $n, m = 0-2$)[a]

	V(X,Y)	V(X)		∪[V(X,H)]		V(Y)		∪V(Y,H)		∪Asyn		
H_nXYH_m	$\bar{N}$	$\bar{N}$	$\langle S_z\rangle$	$\bar{N}$	$\langle S_z\rangle$	$\bar{N}$	$\langle S_z\rangle$	$\bar{N}$	$\langle S_z\rangle$	$\bar{N}$	$\langle S_z\rangle$	$\Delta\mu$
Cl_2	1.0	6.4				6.4						
va		7.4	0.23			7.4	0.23					−1
a(3e)		7.4	0.23			7.4	0.23					−1
HSCl	1.2	4.3		1.89		6.5						
va	0.2 + 0.4	5.0	0.20	1.96	0.03	7.1	0.16			0.1	0.05	+2
a(3e)		5.3	0.30	1.92	0.03	7.6	0.14					−1
H_2PCl	1.4	2.0		4.00		6.5						
va	1.1	2.3	0.08	4.14	0.07	6.9	0.09			0.5	0.20	+1
a(3e)		3.0	0.30	4.10	0.09	7.8	0.08					−1
H_3SiCl	1.5			5.97		6.4						
va	1.5			6.18	0.11	6.6	0.08			0.5	0.22	+1
a(3e)		0.9	0.17	6.22	0.20	7.8	0.10					0
H_2S_2	1.5	4.3		1.91		4.3		1.91				
va	2 × 0.5	4.7	0.11	1.97	0.03	4.7	0.11	1.97	0.03	0.4	0.17	+3
a(3e)		5.5	0.21	1.91	0.02	5.5	0.21	1.91	0.02			−1
H_2PSH	1.6	2.0		4.00		4.3		1.88				
va	1.6	2.1	0.06	4.10	0.06	4.4	0.05	1.91	0.02	0.5	0.23	+3
a(3e)		3.1	0.25	4.10	0.07	5.7	0.14	1.92	0.01			−1
H_3SiSH	1.8			5.96		4.2		1.88				
va	1.8			6.13	0.08	4.3	0.06	1.92	0.04	0.6	0.29	+2
a(3e)		1.2	0.18	6.08	0.14	5.6	0.13	1.95	0.01			0
H_4P_2	1.8	2.1		3.96		2.1		3.96				
va	1.8	2.2	0.04	4.08	0.06	2.2	0.04	4.08	0.06	0.5	0.22	+4
a(3e)		3.4	0.19	4.06	0.04	3.4	0.19	4.06	0.04			−1
H_2PSiH_3	1.9	2.0		3.96				5.98				
va	1.9	2.2	0.06	4.02	0.05			6.15	0.09	0.6	0.26	+2
a	1.2	2.4	0.12	4.04	0.03	1.2	0.17	6.03	0.11			+1
H_6Si_2	1.9			5.95				5.95				
va	1.9			6.07	0.06			6.07	0.06	0.7	0.31	+6
a	2 × 0.5	0.9	0.13	6.05	0.10	0.9	0.13	6.05	0.10			+3

[a] To simplify the discussion, the monosynaptic basins of each given center have been merged. Concerning the protonated basins of a given center, the numbers shown are actually the sum of the integrated property over these basins, as indicated by the ∪ symbol. Similarly, the sum of the integrated property over all the asynaptic basins is reported. For the anionic systems, the basin-integrated spin densities, $\langle S_z\rangle$, are also indicated. These quantities being always negligible for the V(X,Y) basins (<0.01), they are not reported. $\Delta\mu$ is the variation of the morphic number (the number of basins) with respect to the neutral molecule.

TABLE 7: Same as Table 6 but for X = F, O, N, C and Y = Cl, S, P, Si

	V(X,Y)	V(X)		∪V(X,H)		V(Y)		∪V(Y,H)		∪Asyn		
H_nXYH_m	$\bar{N}$	$\bar{N}$	$\langle S_z\rangle$	$\bar{N}$	$\langle S_z\rangle$	$\bar{N}$	$\langle S_z\rangle$	$\bar{N}$	$\langle S_z\rangle$	$\bar{N}$	$\langle S_z\rangle$	$\Delta\mu$
FCl	0.6	6.8				6.3						
va	0.1	7.4	0.14			7.2	0.32					+1
a(3e)		7.4	0.22			7.4	0.25					−1
H_3CCl	1.4			6.07		6.4						
va	1.4			6.18	0.06	6.4	0.03			0.7	0.32	+3
a		0.5	0.14	6.47	0.31	7.9	0.02					0
HSF	0.8	4.3		1.87		6.9						
va	0.6	4.9	0.27	2.00	0.05	7.1	0.08			0.1	0.05	+1
a(3e)		5.3	0.31	1.95	0.03	7.6	0.13					−1
HSOH	1.1	4.3		1.89		4.8		1.72				
va	1.1	4.5	0.08	1.94	0.03	4.8	0.03	1.78	0.03	0.7	0.30	+1
a(3e)		5.5	0.20	1.92	0.02	5.5	0.23	1.77	0.02			−1
H_2NSH	1.6	2.0		4.02		4.2		1.91				
va	1.6	2.1	0.01	4.14	0.05	4.3	0.04	1.94	0.02	0.7	0.35	+2
a		2.9	0.29	4.04	0.18	6.0	0.00	1.88	0.00			−1
H_3CSH	1.6			6.03		4.3		1.89				
va	1.6			6.27	0.12	4.4	0.04	1.92	0.02	0.6	0.29	+3
a		0.5	0.14	6.48	0.30	6.0	0.03	1.90	0.00			0
H_2PF	0.9	2.0		3.98		6.9						
va	0.9	2.3	0.14	4.18	0.10	6.9	0.04			0.5	0.15	+2
a(3e)		3.0	0.31	4.14	0.08	7.7	0.08					−1
H_3CPH_2	1.8			5.96		2.1		4.00				
va	1.8			6.05	0.05	2.1	0.03	4.12	0.07	0.5	0.25	+3
a		0.5	0.13	6.54	0.25	3.7	0.07	4.02	0.01			0

basins, each containing 0.5 *e*, are centered on the axis linking the two sulfur cores, thus characterizing a protocovalent bond in the vertical state. In contrast with the $H_4P_2^-$ type systems, a catastrophe does occur into the region of chemical interactions, which affects the number of the valence basins. Moreover, there is a subsequent transfer of electron density toward the S and S′ lone pairs (2 × 0.4 *e*), associated with a smaller population of the asynaptic basins, whereas each V(H,S) basin still absorbs

TABLE 8: Same as Table 6 but for X = F, O, N, C

H_nXYH_m	V(X,Y)	V(X)		∪V(X,H)		V(Y)		∪V(Y,H)		∪Asyn		
	$\bar{N}$	$\bar{N}$	$\langle S_z\rangle$	$\bar{N}$	$\langle S_z\rangle$	$\bar{N}$	$\langle S_z\rangle$	$\bar{N}$	$\langle S_z\rangle$	$\bar{N}$	$\langle S_z\rangle$	$\Delta\mu$
F_2	2 × 0.2	6.7				6.7						
va		7.4	0.23			7.4	0.23					−2
a(3e)		7.4	0.23			7.4	0.23					−2
H_3CF	1.0			6.09		6.7						
va	1.0			6.18	0.06	6.7	0.01			0.8	0.35	+3
a		0.6	0.18	6.35	0.27	7.8	0.03					0
H_2O_2	0.8	4.8		1.71		4.8		1.71				
va	0.7	4.8	0.02	1.75	0.02	4.8	0.02	1.75	0.02	0.8	0.38	+2
a(3e)		5.7	0.22	1.72	0.02	5.7	0.22	1.72	0.02			−1
H_4N_2	1.4	2.3		3.90		2.3		3.90				
va	1.4	2.3	0.01	3.96	0.03	2.3	0.01	3.96	0.03	0.9	0.41	+4
a(3e)		3.4	0.18	3.94	0.05	3.4	0.18	3.94	0.05			−1

0.07 *e*. Observation of the integrated spin density clearly shows the enhancement of the localization of the unpaired electron into the lone pairs of each sulfur atom, whose contribution to $\langle S_z\rangle$ becomes now dominant. This tendency is accentuated in HSCl (the asynaptic basins bear no more than 10% of the $\langle S_z\rangle$ value) with the expected disymmetry between both moieties (for example, a larger population of the V′(Cl) basin compared to the V′(S) one and a greater localization of the unpaired electron onto the sulfur atom). In H_2PCl no splitting of the V(P,Cl) occurs, probably because the electron transfer toward the lone pairs is smaller than in H_2S_2 and HSCl (and, as a consequence, the population and spin density of the asynaptic basins are still non-negligible). Among the compounds isoelectronic to ClF, only HSF belongs to this set, its bonding population decreasing from 0.8 *e* in the neutral to 0.6 *e* in the vertical anion. Finally, from the value of its vEA, F_2 should also be included in this set, but the expected decrease of the very small amount of its bonding population results actually in its complete transfer toward the lone pairs, so that, as shown below, this molecule behaves actually as Cl_2.

3. In Cl_2, which has a positive vEA (and as a consequence, a positive aEA), the vertical attachment results in the disappearance of the disynaptic V(Cl,Cl′) basin and no asynaptic basin is created. Due to the large electronegativity of the molecule, the monosynaptic basins are able to absorb the V(Cl,Cl′) population plus the extra electron, i.e., 1.0 *e* each. As will be seen shortly, the vertical anion Cl_2^- presents the typical topology of the relaxed anions. Despite its positive vEA, FCl keeps a disynaptic basin in the vertical state, but so weakly populated (0.07 *e*) that the covalent bond can be considered as broken.

Relaxed Anions.

Modification of the ELF Topology. The geometry relaxation, corresponding mainly to a lengthening of the X−Y bond, makes disappear either the disynaptic V(X,Y) basin (as in $H_4P_2^-$) or the monosynaptic V′(X) and V′(Y) basins arising from the splitting of V(X,Y) (as in $H_2S_2^-$), as well as all the asynaptic basins appearing during the vertical attachment (except for Cl_2^-, in which the vertical anion already presents a "3e type" ELF topology). For X = Y, the topology of the 3e-bonded radical anions (Figure 3c) is thus composed by (i) two core basins C(X), (ii) 2*n* protonated V(X,H) basins, and (iii) 6 − 2*n* monosynaptic basins V(X) (2 for Cl_2^-) such that the net variation of the number of basins with respect to the neutral state is $\Delta\mu = -1$. In the framework of the catastrophe theory such a process with $\Delta\mu < 0$ is called *miomorphic*. The localization domain reduction begins by the core/valence reduction (instead of beginning by the core/core reduction as in the neutral state) and leads to a topological system composed of two H_nX fragments. For X ≠ Y the 3e bond formation corresponds also to a *miomorphic* process, except when one of the heavy atoms is a saturated atom (here Si; see Table 6), where the number of basins in the anion is the same as in the neutral ($\Delta\mu = 0$, *tautomorphic* process): indeed, the disappearance of the disynaptic basin is accompanied by the creation of a V(Si) basin, which was nonexistent in the neutral state. For isoelectronic to ClF^- systems (Table 7) or to F_2^- systems (Table 8) the relaxation of the geometry always leads to a *miomorphic* or *tautomorphic* process.[60] Finally, the only radical anions not obeying the $\Delta\mu = -1$ or $\Delta\mu = 0$ rule are $H_2PSiH_3^-$ ($\Delta\mu = +1$) and $H_6Si_2^-$ ($\Delta\mu = +3$): in the former the presence of a disynaptic V(P,Si) basin indicates the keeping of the covalent character of the bond in the anion, in the latter two monosynaptic V′(Si) between the two Si cores are the signature of the protocovalent character of the bond. For these non-3e-bonded systems it is noteworthy that the variation of the X−Y bond length is smaller than for the other isoelectronic to Cl_2^- radical anions.

Transfer of Electron Density and Localization of the Lone Electron. On a quantitative point of view (Tables 6−8), the disappearance of the disynaptic and asynaptic basins results in the transfer of their population toward the monosynaptic basins (the variation of the protonated ones being comparatively very low). In $H_{2n}X_2^-$ compounds, the charge in the monosynaptic basin (5.5 *e* versus 5 *e* for H_2S_2) used in conjunction with the integrated spin density $\langle S_z\rangle$ (0.21 in $H_2S_2^-$) shows that the additional electron is (i) uniformly distributed between both subsystems and (ii) mainly localized into the monosynaptic basins. More precisely, the spin density of the whole H_nX fragment remains constant (0.23), but each added V(X,H) basin carries away a small contribution of 0.02. It is noteworthy that the decrease of the V(X) contribution, Cl_2^- (0.23) → $H_2S_2^-$ (0.21) → $H_4P_2^-$ (0.19), is then nearly proportional to the decrease of the 3e-bond energy (30.7 → 26.0 → 21.0 kcal mol^{-1}). For 3e-bonded radical anions with X ≠ Y, the most electronegative atom tends to close its valence shell, as illustrated by the variation of the V(Cl) population and integrated spin density along the series Cl_2^- → $HSCl^-$ → H_2PCl^-: 7.4 *e*/0.23 → 7.6 *e*/0.14 → 7.8/0.08. This localization of the lone electron into the monosynaptic basins should be corrected when one of the heavy atoms is a saturated atom (see Table 6 for X = Si or Tables 7 and 8 for X = C): indeed, the (dominant) part of the integrated spin density borne by the XH_3 fragment is spread over the V(X) and the three V(X,H) basins, which therefore play the role of a lone pair basin. At this stage, it is noteworthy that the weights of the resonant Lewis structures can be estimated from the $\langle S_z\rangle$ value. For example, in the case of HSCl, if one includes the small V(H,S) contribution into the dominant V(S) ones, one finds:

$$H\dot{S}\cdots\ddot{C}l^-(\sim 70\%) \leftrightarrow H\ddot{S}^-\cdots\dot{C}l(\sim 30\%)$$

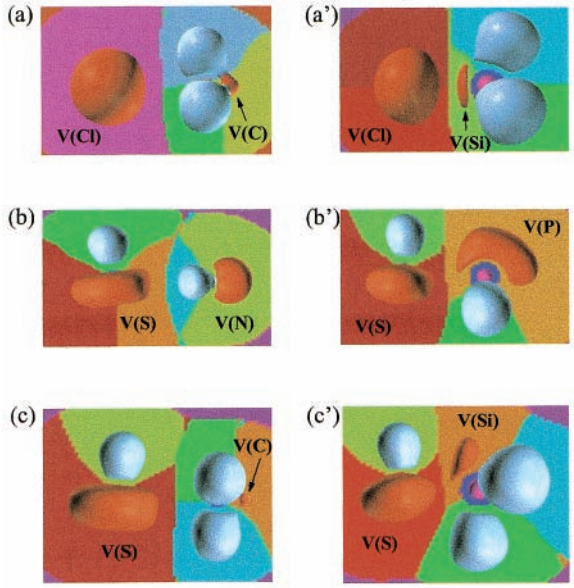

Figure 4. ELF isosurfaces for (a) H_3CCl^-, (b) H_2NSH^-, and (c) H_3CSH^- radical anions and their isoelectronic to Cl_2^- counterparts, (a′) H_3SiCl^-, (b′) H_2PSH^-, and (c′) H_3SiSH^-. Color code: magenta = core, red = valence monosynaptic, blue = valence protonated. The basin partition maps in the plane of symmetry of the compounds are also shown.

thereby establishing a quantitative correspondence between the VB and topological descriptions of the 3e bond.

Toward a General Topological Signature of the 3e Bond. For some of the investigated compounds (H_3CF, H_3CCl, H_2NSH, H_3CSH, H_3CPH_2), the increase of the bond distance upon electron attachment is much larger than for the other members of their series (up to twice larger) and, except for H_2NSH^-, the associated binding energies are smaller than 3.3 kcal mol^{-1} (see Tables 2 and 3). These energetic and structural criteria are enough to eliminate the related anions from the 3e-bonded molecules group. However, it is interesting to analyze in detail their ELF topology, to refine our characterization of the 3e bond. First of all, these compounds undergo the disappearance of the V(X,Y) basin upon electron attachment, but an important difference with their isoelectronic to Cl_2^- counterparts arises, concerning the connectivity of the V(X) and V(Y) attractors, as illustrated by Figure 4: in the latter group of anions the monosynaptic basins of the two moieties do share a common separatrice, localized between the cores of the heavy atoms, whereas they *do not* in the former group. The topology of the very low bounded compounds is then typically those of systems that are "on the way toward the dissociation". The electron attachment still gives rise to a transfer of electron density toward the lone pair basins, *but the extra electron is actually nearly exclusively localized on the most electronegative H_nX moiety, for which the spin density is therefore negligible* (see Tables 7 and 8). For instance, for the most localized system, H_2NSH^-, the integrated basin spin densities and basin populations accredit the following VB description: $HS^-\cdots H_2N^\bullet$.

IV.B.2. Analysis of the Electron Delocalization. Up to now we have only discussed the electron *localization* in some 3e-bonded radical anions. However, as stressed by Hiberty et al.,[7] "the three-electron bond is nothing but a pure fluctuation of an electronic charge from one fragment to another". Unfortunately, the MO or VB descriptions of such bonds do not provide any direct measure of this fluctuation. One a posteriori verifies, considering some structural properties as equilibrium geometry or dissociation energy or through the value of the VB resonance energy, that this phenomenon is correctly taken into account. In contrast, starting from a given quantum mechanical calculation of the molecule, the topological analysis of the ELF gradient field allows us to characterize, as described in section II, directly and *quantitatively* the electron delocalization for each molecular basin.

TABLE 9: Population of the Monosynaptic $V(X_1)$ Basin, $\bar{N}$, Standard Deviation, $\sigma(\bar{N})$, Relative Fluctuation, $\lambda(\bar{N})$, and Contribution of Other Basins (%) to $\sigma^2(\bar{N})$ for the $H_{2n}X_2$ Molecule and $H_{2n}X_2^-$ Radical Anion (va = Vertical Anion, A(3e) = Relaxed 3-Electron-Bonded Anion)

compd	$\bar{N}$	$\sigma(\bar{N})$	$\lambda(\bar{N})$	contribution analysis
H_4P_2	2.1	0.8	0.41	$V(H_1,P_1)$ 24%, $V(P_1,P_2)$ 21%, $C(P_1)$ 20%, $V(P_2)$ 6%
va	2.2	1.0	0.43	$V(H_1,P_1)$ 23%, $V(P_1,P_2)$ 19%, $C(P_1)$ 19%, $V(P_2)$ 6%
a(3e)	3.4	1.1	0.38	$V(H_1,P_1)$ 29%, $C(P_1)$ 21%, $V(P_2)$ 16%
H_2S_2	4.3	1.2	0.32	$V(H_1,S_1)$ 34%, $C(S_1)$ 25%, $V(S_1,S_2)$ 24%, $V(S_2)$ 12%
va	4.7	1.2	0.32	$V(H_1,S_1)$ 34%, $C(S_1)$ 23%, $V'(S_1)$ 14%, $V(S_2)$ 14%
a(3e)	5.5	1.2	0.25	$V(H_1,S_1)$ 45%, $C(S_1)$ 30%, $V(S_2)$ 21%
Cl_2	6.4	1.1	0.19	$C(Cl_1)$ 42%, $V(Cl_1,Cl_2)$ 26%, $V(Cl_2)$ 30%
va	7.4	1.1	0.16	$V(Cl_2)$ 50%, $C(Cl_1)$ 47%
a(3e)	7.4	0.9	0.12	$V(Cl_2)$ 38%, $C(Cl_1)$ 60%

Considering that the formation of a 3e bond in H_nXYH_m systems upon electron attachment is accompanied by a transfer of electron density toward the lone pair basins V(X) and V(Y), one is induced to think that the electron fluctuation responsible for the stability of the 3e bond takes place principally between these basins. As a first step of the understanding of electron delocalization in $H_nXYH_m^-$ systems, one might thus consider the relative fluctuation λ of the monosynaptic basin populations. This quantity is presented in Table 9 for the three $H_{2n}X_2$ systems isoelectronic to Cl_2 and their anions. It is noteworthy that, in the following analysis, the lone pair basins of each given center have been merged because we are only interested by their fluctuation as a whole. Surprisingly, one observes that λ decreases from the neutral to the vertical anion and then to the relaxed anion: this is a consequence of the near constancy (or the very small increase for H_4P_2) of the variance, associated with a subsequent increase of the basin population. More relevant and more informative for the investigated systems is the evolution of the contribution of the $V(X_2)$ basin to the $V(X_1)$ variance, i.e., the relative $B_{V(X_1),V(X_2)}$ (and vice versa). In the neutral systems, this contribution increases from 6% in H_4P_2 to 29% in Cl_2 (this confirms the covalent character of the bonding in H_4P_2, whereas proper description of the bonding in Cl_2 should involve ionic structures such as Cl^+Cl^-, which ensures a delocalization between lone pair basins). But more interesting is the evolution of the same contribution from the neutral to the vertical anion and then to the relaxed 3e-bonded anion. Under vertical attachment, one observes that it is related to the transfer of population from the $V(X_1,X_2)$ to the $V(X_i)$ basins: it is not significant for H_4P_2, small for H_2S_2 and very large for Cl_2, in which it reaches 50%. Under relaxation of the geometry, the variations of the relative $B_{V(X_1),V(X_2)}$ are still related to the transfer of the electronic density toward the lone pair basins. One observes:

- A large increase in $H_4P_2^-$ (but from 6 to only 16%), corresponding to the transfer of all the $V(X_1,X_2)$ population and of the extra electron density toward the lone pair basins.
- A moderate increase in $H_2S_2^-$ (from 14 to 21%), because one part of the transfer has already been achieved during the vertical attachment.

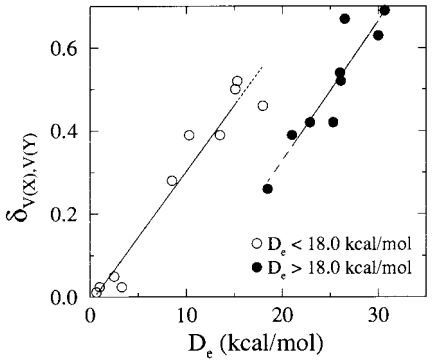

Figure 5. Index of delocalization $\delta_{V(X),V(Y)}$, as defined in eq 8, plotted as a function of the three-electron bond dissociation energies D_e.

•A *decrease* in Cl_2^- (from 50 to 38%), because the relaxation is nothing but a lengthening of the bond, the transfer being carried out during the vertical attachment.

However, if we compare the relative $B_{V(X_1),\,V(X_2)}$ of the three $H_{2n}X_n^-$ anions, we see that, as expected, it increases from $H_4P_2^-$ to Cl_2^-, as the dissociation energy does. Indeed, the VB description of 3e-bonded systems (and more generally of hemibonded systems) shows that the fluctuation of the electronic charge between the two fragments involved in the bond increases with the resonance energy, i.e., with the overlap of the lone pair orbitals. It is thus worth considering whether a correlation exists between the electron delocalization as defined in the topological theory of the chemical bond and the dissociation energy of the 3e-bonded radical anions (which is, in a reasonable approximation, proportional to the resonance energy). The relevant topological quantity to consider is the delocalization index given by eq 8, with $\Omega_a = V(X)$ and $\Omega_b = V(Y)$ (where, as already mentioned, the lone pair basins of each given center have been merged):

$$\delta_{V(X),V(Y)} = B_{V(X),V(Y)} + B_{V(Y),V(X)} = 2B_{V(X),V(Y)} \qquad (9)$$

The δ index is plotted in Figure 5 for all investigated systems, as a function of their dissociation energy D_e. A rather good linear correlation is obtained if one separates the anions into two groups, depending on whether D_e is smaller or greater than 18 kcal mol^{-1}. It is noteworthy that this value corresponds more or less to the one generally given for the lower bound of the 3e bond dissociation energy (15−20 kcal mol^{-1}). Except for three of them (H_2PF^-, HSF^-, and ClF^-), the most strongly bonded radical anions group consists of all the symmetrical systems (as clear from the classical MO scheme, perturbation is maximum for degenerate levels).

IV.B.3. Topological versus MO/Linnett/VB Type Descriptions of the 3e Bond. The disappearance of the disynaptic basin upon formation of the 3e bond could be related to the destabilizing effect of the additional antibonding electron, in the context of the MO description of the 3e bond (see panel 1 of Figure 1). However, to have a deeper insight into the physical origin of this process, it is worthy to investigate the topology of another type of odd-electron bond having a formal bond order of $^1/_2$, the one-electron bond. For the radical cations of the $H_nX_2^+$ type with (X, *n*) = (Li, 0), (Be, 2), (B, 4), (C, 6), the one-electron bond is characterized by a disynaptic basin V(X,X), with a population ranging from 1 *e* in Li_2^+ to 0.4 *e* in $C_2H_6^+$.[61] Thus, considering the Linnett description of the 3e bond (see panel 2 of Figure 1), the lack of disynaptic basin should be attributed to the Pauli repulsion between the a and b same-spin (α) electrons, which counteracts the bonding effect of the Ψ_{ab} (β) electron. The role of the Pauli repulsion in 3e bonds has also been emphasized by Bieckelhaupt et al. in the context of their energy decomposition scheme for open-shell systems.[14] Finally, the local picture provided by the topological method can more easily be connected with the compact VB description of the 3e bond (as shown, for example, by its ability to provide the weights of the two limiting Lewis structures involved in a VB treatment).

V. Conclusion

The results presented in this paper show that the topological description of the chemical bond provides a new insight into the bonding evolution upon electron attachment, giving rise to a 3e-bonded radical anion. The changes occurring in the number and the population of valence basins, on one hand, are consistent with the descriptions in terms of delocalized MO or resonance structures and, on the other hand, provide a chemical picture of the electron cloud reorganization. In short, the topological signatures obtained for 3e-bonded radical anions of the $H_nXYH_m^-$ type (which could be adapted for 3e-bonded radical cations) are

1. the absence of V(X,Y) disynaptic basin
2. the transfer of the extra electron and of the population initially into the bonding region toward the V(X) and V(Y) monosynaptic basins
3. the balanced localization of the spin density into these monosynaptic basins
4. the sharing of a common separatrice between the V(X) and V(Y) basins
5. the classification of the anions into two groups, depending on whether their dissociation energy is smaller or greater than 18 kcal mol^{-1} (a roughly linear increase of the delocalization index on the dissociation energy is observed within each of these two groups)

It is noteworthy that the electron cloud reorganization following electron attachment can be somehow hampered by conservation of the geometry (vertical processes). The removal of this constraint by relaxation enables the disappearance of the bonding basin and the localization of the spin density into the lone pair regions. Similar trends have already been found in radicals such as monochloride oxides ClO_n[36] or in carbonyl compounds in their neutral triplet, radical anion, and cation states.[35] One of the outlooks of this work would be to interpret the latter phenomena within the catastrophe theory framework.

References and Notes

(1) Dohjan, J. G.; Chen, E. C. M.; Wentworth, W. E. *J. Phys. Chem.* **1996**, *100*, 9649.
(2) Pauling, L.; MacClure, V. *J. Am. Chem. Soc.* **1931**, *53*, 3225.
(3) Pauling, L. *The Nature of the Chemical Bond*; Cornell University Press: Ithaca, NY, 1948.
(4) Braıda, B.; Hiberty, P. *J. Phys. Chem. A* **2000**, *104*, 4618.
(5) Hiberty, P. C.; Berthe-Gaujac, N. *J. Phys. Chem. A* **1998**, *102*, 3169.
(6) Harcourt, R. D. *J. Phys. Chem. A* **1997**, *101*, 2496; Erratum. *J. Phys. Chem. A* **1997**, *101*, 5962.
(7) Hiberty, P. C.; Humbel, S. *J. Phys. Chem.* **1994**, *98*, 11697.
(8) Hiberty, P. C.; Humbel, S.; Danovich, D.; Shaik, S. *J. Am. Chem. Soc.* **1995**, *117*, 9003.
(9) Gill, P. M. W.; Radom, L. *J. Am. Chem. Soc.* **1988**, *110*, 4931.
(10) Clark, T. *J. Am. Chem. Soc.* **1988**, *110*, 1672.
(11) Komiha, N.; Daudey, J. P.; Malrieu, J. P. *J. Phys. B* **1987**, *20*, 4375.
(12) Humbel, S.; Hoffmann, N.; Côte, I.; Bouquant, J. *Chem. Eur. J.* **2000**, *6*, 1592.
(13) Nichols, L. S.; Illies, A. J.; *J. Am. Chem. Soc.* **1999**, *121*, 9176 and references therein.
(14) Bickelhaupt, F. M.; Diefenbach, A.; de Visser, S. P.; de Konig, L. J.; Nibbering, N. M. M. *J. Phys. Chem. A* **1998**, *102*, 9549.
(15) Braıda, B.; Hiberty, P.; Savin, A. *J. Phys. Chem. A* **1998**, *102*, 7872.

(16) Dézarnaud-Dandine, C.; Sevin, A. *J. Am. Chem. Soc.* **1996**, *118*, 4427.
(17) Humbel, S.; Demachy, I.; Hiberty, P. C. *Chem. Phys. Lett.* **1995**, *247*, 126.
(18) Harcourt, R. D. *Eur. J. Inorg. Chem.* **2000**, pp 1901−1916.
(19) Harcourt, R. D. *J. Chem. Educ.* **1985**, *99*, 99.
(20) Linnett, J. W. *The Electronic Structure of Molecules*; Methuen & CO LTD: London, 1964.
(21) Hiberty, P. C.; Humbel, S.; Byrman, C. P.; van Lenthe, J. H. *J. Chem. Phys.* **1994**, *101*, 5969.
(22) Lewis, G. N. *Valence and the Structure of Atoms and Molecules*; Dover: New York, **1966**.
(23) Gillespie, R. *Molecular Geometry*; Van Nostrand Reinhold: London **1972**.
(24) Gillespie, R. J.; Robinson, E. A. *Angew. Chem., Int. Ed. Engl.* **1996**, *35*, 495.
(25) Bader, R. F. W. *Atoms in Molecules: A Quantum Theory*; Oxford University Press: Oxford, 1990.
(26) Bader, R. F. W.; MacDougall, P. J.; Lau, C. D. H. *J. Am. Chem. Soc.* **1984**, *106*, 1594.
(27) Bader, R. F. W.; Gillespie, R. J.; MacDougall, P. J. *J. Am. Chem. Soc.* **1988**, *110*, 7329.
(28) Bader, R. F. W.; Johnson, S.; Tang, T.-H.; Popelier, P. L. A. *J. Phys. Chem.* **1996**, *100*, 15398.
(29) MacDougall, P. J. The Laplacian of the Electronic Charge Distribution. Ph.D. Thesis, McMaster University, Hamilton Ontario Canada, February 1989.
(30) Bader, R. F. W.; MacDougall, P. J. *J. Am. Chem. Soc.* **1985**, *107*, 6788.
(31) Silvi, B.; Savin, A. *Nature* **1994**, *371*, 683.
(32) Becke, A. D.; Edgecombe, K. E. *J. Chem. Phys.* **1990**, *92*, 5397.
(33) Savin, A.; Nesper, R.; Wengert, S.; Fässler, T. F. *Angew. Chem., Int. Ed. Engl.* **1997**, *36*, 1809.
(34) Noury, S.; Colonna, F.; Savin, A.; Silvi, B. *J. Mol. Struct.* **1998**, *450*, 59.
(35) Fourré, I.; Silvi, B.; Chaquin, P.; Sevin, A. *J. Comput. Chem.* **1990**, *93*, 2992.
(36) Beltrán, A.; Andrés, J.; Noury, S.; Silvi, B. *J. Phys. Chem. A* **1999**, *103*, 3078.
(37) Llusar, R.; Beltràn, A.; Juan Andrès, S. N.; Silvi, B. *JCC* **1999**, *20*, 1517.
(38) Berski, S.; Silvi, B.; Latajka, Z.; Leszczyński, J. *J. Chem. Phys.* **1999**, *111*, 2542.
(39) Krokidis, X.; Moriarty, N. W.; William, A.; Lester, J.; Frenklach, M. *Chem. Phys. Lett.* **1999**, pp 534−542.
(40) Chevreau, H.; Sevin, A. *Chem. Phys. Lett.* **2000**, *322*, 9.
(41) Silvi, B.; Gatti, C. *J. Phys. Chem. A* **2000**, *104*, 947.
(42) Fuster, F.; Sevin, A.; Silvi, B. *J. Phys. Chem. A* **2000**, *104*, 852.
(43) Fuster, F.; Sevin, A.; Silvi, B. *J. Comput. Chem.* **2000**, *21*, 509.
(44) Fuster, F.; Silvi, B.; Berski, S. Latajka, Z. *J. Mol. Struct.* **2000**, *555*, 75.
(45) Chesnut, D. B.; Bartolotti, L. J. *Chem. Phys.* **2000**, *253*, 1.
(46) Chamarro, E.; Santos, J. C.; Gómez, B.; Contreras, R.; Fuentealba, P. *J. Chem. Phys.* **2001**, *114*, 23.
(47) Krokidis, X.; Noury, S.; Silvi, B. *J. Phys. Chem. A* **1997**, *101*, 7277.
(48) Krokidis, X.; Silvi, B.; Dézarnaud-Dandine, C.; Sevin, A. *New J. Chem.* **1998**, *22*, 1341.
(49) Bergès, J.; Fuster, F.; Silvi, B.; Jacquot, J. P.; Houée-Levin, C.; *Nukleonika* **2000**, *45*, 23.
(50) Abraham, R.; Marsden, J. E. *Dynamics the Geometry of Behavior*; Addison-Wesley: Reading, MA, 1992.
(51) Burdett, J. K.; McCormick, T. A. *J. Phys. Chem. A* **1998**, *102*, 6366.
(52) Bader, R. F. W. In *Localization and Delocalization in quantum Chemistry*; Chalvet, O., Daudel, R., Diner, S., Malrieu, J. P., Eds.; Reidel: Dordrecht, The Netherlands, 1975; Vol. I, pp 15−38.
(53) Fradera, X.; Austen, M. A.; Bader, R. F. W. *J. Phys. Chem.* **1999**, *103*, 304.
(54) Chesnut, D. B.; Bartolotti, L. J. *Chem. Phys.* **2000**, *257*, 175.
(55) Ángyán, J. G.; Loos, M.; Mayer, I. *J. Phys. Chem.* **1994**, *98*, 5244.
(56) Cioslowski, J.; Mixon, S. T. *J. Am. Chem. Soc.* **1991**, *113*, 4142.
(57) Frisch, M. J.; Trucks, G. W.; Schlegel, H. B.; Gill, P. M. W.; Johnson, B. G.; Robb, M. A.; Cheeseman, J. R.; Keith, T.; Petersson, G. A.; Montgomery, J. A.; Raghavachari, K.; Al-Laham, M. A.; Zakrzewski, V. G.; Ortiz, J. V.; Foresman, J. B.; Cioslowski, J.; Stefanov, B. B.; Nanayakkara, A.; Challacombe, M.; Peng, C. Y.; Ayala, P. Y.; Chen, W.; Wong, M. W.; Andres, J. L.; Replogle, E. S.; Gomperts, R.; Martin, R. L.; Fox, D. J.; Binkley, J. S.; Defrees, D. J.; Baker, J.; Stewart, J. P.; Head-Gordon, M.; Gonzalez, C.; Pople, J. A. *Gaussian 94*, revision D.4; Gaussian Inc.: Pittsburgh, PA, 1995.
(58) Noury, S.; Krokidis, X.; Fuster, F.; Silvi, B. *Comput. Chem.* **1999**, *23*, 597.
(59) The ELF value at these attractors being lower than 0.8, the corresponding localization domains are not seen in Figure 3.
(60) Because of the protocovalent character of the bond the $\Delta\mu = -1$ rule is replaced by $\Delta\mu = -2$ for the $F_2 + e \rightarrow F_2^-$ reaction.
(61) The one-electron-bonded radical cation H_2^+ constitutes a particular case since it is also a one-electron system: ELF equals 1.0 everywhere.
(62) Linnett, J. W. J. *J. Am. Chem. Soc.* **1961**, *83*, 2643.